From Blood Oxygenation Level Dependent (BOLD) signals to brain temperature maps

Roberto C. Sotero[1,2] and Yasser Iturria-Medina[3]

[1]National Bioinformatics Center (BIOINFO). InSTEC. Havana. Cuba

[2]Montreal Neurological Institute Brain Imaging Centre
Depts. of Neurology and Neurosurgery and Biomedical Engineering
McGill University Montreal, Quebec, Canada

[3]Cuban Neuroscience Center. Havana. Cuba

Correspondence to: roberto.soterodiaz@mcgill.ca

Nature Precedings : hdl:10101/npre.2010.4772.1 : Posted 13 Aug 2010

Nature Precedings : hdl:10101/npre.2010.4772.1 : Posted 13 Aug 2010

Abstract

A theoretical framework is presented for converting Blood Oxygenation Level Dependent (BOLD) images to temperature maps, based on the idea that disproportional local changes in cerebral blood flow (*CBF*) as compared with cerebral metabolic rate of oxygen consumption ($CMRO_2$) during functional brain activity, lead to both brain temperature changes and the BOLD effect. Using an oxygen limitation model and a BOLD signal model we obtain a transcendental equation relating *CBF* and $CMRO_2$ changes with the corresponding BOLD signal, which is solved in terms of the Lambert *W* function. Inserting this result in the dynamic bio-heat equation describing the rate of temperature changes in the brain, we obtain a non autonomous ordinary differential equation that depends on the BOLD response, which is solved numerically for each brain voxel. In order to test the method, temperature maps obtained from a real BOLD dataset are calculated showing temperature variations in the range: (-0.15, 0.1) which is consistent with experimental results. The method could find potential clinical uses as it is an improvement over conventional methods which require invasive probes and can record only few locations simultaneously. Interestingly, the statistical analysis revealed that significant temperature variations are more localized than BOLD activations. This seems to exclude the use of temperature maps for mapping neuronal activity as areas where it is well known that electrical activity occurs (such as V5 bilaterally) are not activated in the obtained maps. But it also opens questions about the nature of the information processing and the underlying vascular network in visual areas that give rise to this result.

Nature Precedings : hdl:10101/npre.2010.4772.1 : Posted 13 Aug 2010

1. Introduction

The balance between metabolic heat production (due to the oxidation of glucose), heat removal by cerebral blood flow (CBF), and conductive heat loss from the region of interest (ROI) to neighbouring regions, characterize the temperature dynamics in the ROI (Trübel et al., 2006). Thus, it has been proposed (Yablonskiy et al., 2000) that disproportional changes in cerebral metabolic rate of oxygen consumption $(CMRO_2)$ and CBF evoked by neuronal activity can explain the variation in brain tissue temperature (in the range of $\pm 0.2\,^0C$) revealed by functional studies in humans (Yablonskiy et al., 2000; Shevelev et al., 1993; Gorbach et al., 2003) and animals (Trübel et al., 2006; Serota and Gerard, 1938; McElligot and Melzack, 1967; Melzack and Casey, 1967; Hayward and Baker, 1968; LaManna et al., 1989; Gorbach, 1993; Shevelev and Tsicalov, 1997; Shevelev, 1998).

Conventional methods for measuring brain temperatures require invasive probes and can monitor only one or a few locations simultaneously (Le Bihan, 1995). Clearly, a reliable non-invasive method is highly desirable and could have many clinical uses. Non-invasive methods like microwave or infrared based measurements allow temperature to be measured only to a limited depth. Compared to them, magnetic resonance (MR) imaging has the advantage of producing three-dimensional anatomic images of any part of the body in any orientation with high resolution, and the frequency of the MR signal is temperature dependent (Hindman, 1966). It has been demonstrated that this effect can be used for estimating tissue temperature changes (Parker et al., 1983; Kuroda, 1996). On the other hand, changes in the MR imaging (MRI) signal intensity due to blood oxygenation level-dependent (BOLD) contrast (Bandettini et al., 1992; Frahm et al., 1992; Kwong et al., 1992; Ogawa et al., 1992), i.e., the functional MRI (fMRI) signal, is currently the most widely used signal for brain mapping and studying the neural basis

of human cognition. The origin of the BOLD effect is that haemoglobin is diamagnetic when oxygenated and paramagnetic when deoxygenated. Thus, the presence of deoxyhaemoglobin produces a slight alteration in the local MR signal. Then, the larger increase in CBF than $CMRO_2$ following neuronal activity results in a net decrease of the amount of deoxyhaemoglobin present, which produces an increase in the MR signal, the BOLD response (Buxton et al., 2004). Since both BOLD and temperature responses have the same common origin in CBF and $CMRO_2$ changes, it is tempting to propose a model for coupling them.

In this paper, we rewrite the coupling between oxygen consumption and cerebral blood flow given by the oxygen limitation model (Buxton and Frank, 1997) as a gamma function. When substituting this new equation in the BOLD signal model of Davis et al (1998) we obtain a transcendental equation relating CBF and BOLD responses, which is solved in terms of the Lambert *W* function (Corless et al., 1996). Thus, given the BOLD signals we are able to calculate the underlying CBF and $CMRO_2$ changes. These equations for CBF and $CMRO_2$ as functions of the BOLD signal, are inserted in the dynamic bio-heat equation Pennes, 1948; Yablonskiy et al., 2000; Trübel et al., 2006) that describes the rate of temperature changes in the ROI. If we have the BOLD time series for each brain voxel, then we can calculate the corresponding temperature response by solving numerically a non-autonomous differential equation. In this paper we investigate with simulations the temperatures responses associated to different BOLD time series. We also show temperature maps calculated from real BOLD data (Büchel and Friston, 1997).

Nature Precedings : hdl:10101/npre.2010.4772.1 : Posted 13 Aug 2010

Nature Precedings : hdl:10101/npre.2010.4772.1 : Posted 13 Aug 2010

2. Model development

2.1 Modelling temperature changes

The dynamic bio-heat equation describes the rate of temperature change in the brain, $\dot{T}(t)$, when the resting state is disturbed by global changes in blood flow, incoming blood temperature, or oxygen consumption (Pennes, 1948; Yablonskiy et al., 2000; Trübel et al., 2006):

$$C_t\dot{T}(t) = \left(\Delta H^\circ - \Delta H_b\right) CMRO_2\big|_0\, m(t) - \rho_B C_B\, CBF\big|_0\, f(t)\left(T(t) - T_a\right) - \\ - \frac{C_t}{\tau}\left(1 - e^{-\frac{t}{\tau}}\right)\left(T(t) - T_0\right) \qquad (1)$$

where $m(t)$ and $f(t)$ are $CMRO_2$ and CBF normalized to rest, respectively. The physiological interpretation and values of the parameters of this equation are shown in Table 1. The first term at the right side of equation (1) accounts for the amount of heat locally generated per gram of brain tissue per minute due to the oxidation of glucose from which most of the energy required for brain activity is generated. The second term is the rate of heat removal from brain tissue by cerebral blood flow, and the third term describes conductive heat loss within brain tissue (Trübel et al., 2006). By substituting $\dot{T} = 0$ in (1) we found the temperature at rest (T_0):

$$T_0 = T_a + \frac{\left(\Delta H^\circ - \Delta H_b\right)}{\rho_B C_B} \frac{CMRO_2\big|_0}{CBF\big|_0} \qquad (2)$$

If $E(t)$ is the oxygen extraction fraction, that is, the ratio of oxygen consumption to oxygen delivered, then the following equation holds (Buxton et al., 2004):

$$m(t) = f(t)\frac{E(t)}{E_0} \qquad (3)$$

where E_0 is the oxygen extraction fraction at rest. Several works have modelled the relationship between $m(t)$ and $f(t)$ (Buxton and Frank, 1997; Hyder et al., 1998; Vafaee and Gjedde,

Nature Precedings : hdl:10101/npre.2010.4772.1 : Posted 13 Aug 2010

2000; Zheng et al., 2002; Takuya et al., 2003). Particularly, the oxygen limitation model proposed by Buxton and Frank (1997) has been widely employed as part of biophysical models of the generation of the BOLD signal (Buxton et al., 1998; Friston et al., 2000; Friston et al., 2003; Babajani and Zoltanian-Zadeh, 2006; Riera et al., 2006; Riera et al., 2007; Babajani et al., 2008; Blockley et al., 2009):

$$E(f) = 1 - (1 - E_0)^{\frac{1}{f(t)}} \tag{4}$$

Nevertheless, in order to solve the transcendental equation (3) for $f(t)$, is necessary to write (4) in a more suitable way. For this, we generated $E(t)$ data using equation (4) and adjusted to it the gamma function (5) for a f range of $[0.7-2]$:

$$\frac{E(f)}{E_0} = af^{c}(t)e^{-bf(t)} \tag{5}$$

Estimated values for *a*, *b*, and *c* are displayed in Table 1. With this approximation, the relationship between oxygen consumption and blood flow given by (3) becomes:

$$m(t) = af^{c+1}(t)e^{-bf(t)} \tag{6}$$

BOLD signal changes $\frac{\Delta S}{S_0}$ can be expressed in terms of $f(t)$ and $m(t)$ as (Davis et al., 1998):

$$\frac{\Delta S(t)}{S_0} = \frac{S(t) - S_0}{S_0} = A\left(1 - f^{\alpha-\beta}(t)m^{\beta}(t)\right) \tag{7}$$

Substituting (6) in (7) and rearranging terms:

$$f(t)e^{-\frac{b\beta}{\alpha+\beta c}f(t)} = \left(\frac{\left(A - \frac{\Delta S(t)}{S_0}\right)}{Aa^{\beta}}\right)^{\frac{1}{\alpha+\beta c}} \tag{8}$$

Multiplying both sides by $-\frac{b\beta}{\alpha+\beta c}$:

$$-\frac{b\beta}{\alpha+\beta c} f(t) e^{-\frac{b\beta}{\alpha+\beta c} f(t)} = -\frac{b\beta}{\alpha+\beta c} \left(\frac{\left(A - \frac{\Delta S(t)}{S_0} \right)}{A a^{\beta}} \right)^{\frac{1}{\alpha+\beta c}} \tag{9}$$

This is a transcendental equation. For obtaining an analytic solution for $f(t)$ we use the fact that an equation of the form:

$$z e^{z} = x \tag{10}$$

has solution in terms of the Lambert *W* function (Corless et al., 1996):

$$z = W(x) \tag{11}$$

This function is implemented in softwares like Maple, Matlab and Mathematica.

Using this, $f(t)$ can be obtained from equation (9) as:

$$f(t) = -\frac{\alpha+\beta c}{b\beta} W\left(y(t) \right) \tag{12}$$

where $y(t)$ is a function of the BOLD signal:

$$y(t) = -\frac{b\beta}{\alpha+\beta c} \left(\frac{\left(A - \frac{\Delta S(t)}{S_0} \right)}{A a^{\beta}} \right)^{\frac{1}{\alpha+\beta c}} \tag{13}$$

Using equations (6) and (12)-(13), oxygen consumption and blood flow time series are calculated from the corresponding BOLD signal. Then, the temperature in a brain voxel can be obtained from the associated BOLD signal by solving numerically the following non autonomous ordinary differential equation:

Nature Precedings : hdl:10101/npre.2010.4772.1 : Posted 13 Aug 2010

$$\dot{T}(t) + p(t)T(t) = g(t) \tag{14}$$

with initial condition given by (2), and $p(t)$ and $g(t)$ given by:

$$p(t) = -\frac{\rho_B C_B \, CBF\big|_0 (\alpha + \beta c)}{b\beta C_{tissue}} W\left(y(t)\right) \tag{15}$$

$$g(t) = a\frac{CMRO_2\big|_0 \left(\Delta H^\circ - \Delta H_b\right)}{C_{tissue}}\left(-\frac{\alpha+\beta c}{b\beta}W\left(y(t)\right)\right)^{c+1} e^{\frac{\alpha+\beta c}{\beta}W(y(t))} + \\ + T_{arterial}\, p(t) \tag{16}$$

An alternative solution to equation (14) is given in integral form by:

$$T(t) = \frac{1}{\mu(t)}\left(T_0 + \int_0^t \mu(\lambda)\, g(\lambda)\, d\lambda\right) \tag{17}$$

where:

$$\mu(t) = e^{\int_0^t p(\omega) d\omega} \tag{18}$$

3. Results

In this section we first use computational simulations to explore the temperature temporal dynamics associated to different BOLD time series. After that, we show temperature maps calculated from actual BOLD data.

3.1 From simulated BOLD data to temperature time series

In this paper we propose that the temperature temporal response $T(t)$ can be obtained from the BOLD time series by solving the ordinary differential equation (14). We solve this equation numerically with the fourth order Runge-Kutta method. All the parameters values needed are displayed in Table 1. The simulated BOLD data were generated with a step size of $0.1s$ using

Nature Precedings : hdl:10101/npre.2010.4772.1 : Posted 13 Aug 2010

the Metabolic/Hemodynamic Model (MHM) proposed in Sotero and Trujillo-Barreto (2007) with the standard parameters set used in that paper.

Table 1. Values and physiological interpretation of the parameters.

Parameter	Interpretation	Value
C_{tissue}	Tissue heat capacity	$3.664\,\mathrm{J/(gK)}$
ΔH^0	Enthalpy released in the oxidation of glucose: $C_6H_{12}O_6 + 6O_2 \rightarrow 6CO_2 + 6H_2O$	$4.7 \cdot 10^5\,\mathrm{J}$
ΔH_b	Enthalpy used for releasing oxygen from hemoglobin	$2.8 \cdot 10^4\,\mathrm{J}$
$CMRO_2\|_0$	Cerebral metabolic rate of oxygen consumption at rest	$0.0263 \cdot 10^{-6}\ \mathrm{mol/(gs)}$
$CBF\|_0$	Cerebral blood flow at rest	$0.0093\,\mathrm{cm^3/(gs)}$
E_0	Oxygen extraction fraction at rest	0.4
C_B	Blood heat capacity	$3.894\,\mathrm{J/(gK)}$
ρ_B	Blood density	$1.05\,\mathrm{g/cm^3}$
A	Maximum BOLD signal change that could occur corresponding to complete removal of deoxyhemoglobin from the voxel	0.22
α	Steady state flow-volume relation	0.4
β	Parameter dependent on the field strength	1.5
T_a	Arterial blood temperature	$309.15\,K$
a, b, c	Parameters of the gamma function fitted from the $E(f)$ **vs** f curve	0.1870, 0.1572 and -0.6041

Figure 1 displays in the same column the positive BOLD responses (PBRs) and the associated $CMRO_2$ normalized to baseline (m), CBF normalized to baseline (f) and the variation with

Nature Precedings : hdl:10101/npre.2010.4772.1 : Posted 13 Aug 2010

respect to baseline of the temperature (ΔT) . In the case of PBRs, we found they are associated with a decrease in brain temperature. On the other hand, negative BOLD responses (NBRs) are associated with increases in brain temperature (Figure 2). That is, the assumption that CBF is always greater than $CMRO_2$ (imposed by the oxygen limitation model) leads to the conclusion that the sign of temperature is always opposite to the sign of CBF changes. In the case of PBRs, CBF increases (see Figure 1), and this evokes a decrease in temperature. In the case of NBRs we found that both $CMRO_2$ and CBF decrease (in agreement with Shmuel et al., 2002) which leads to an increase in the temperature.

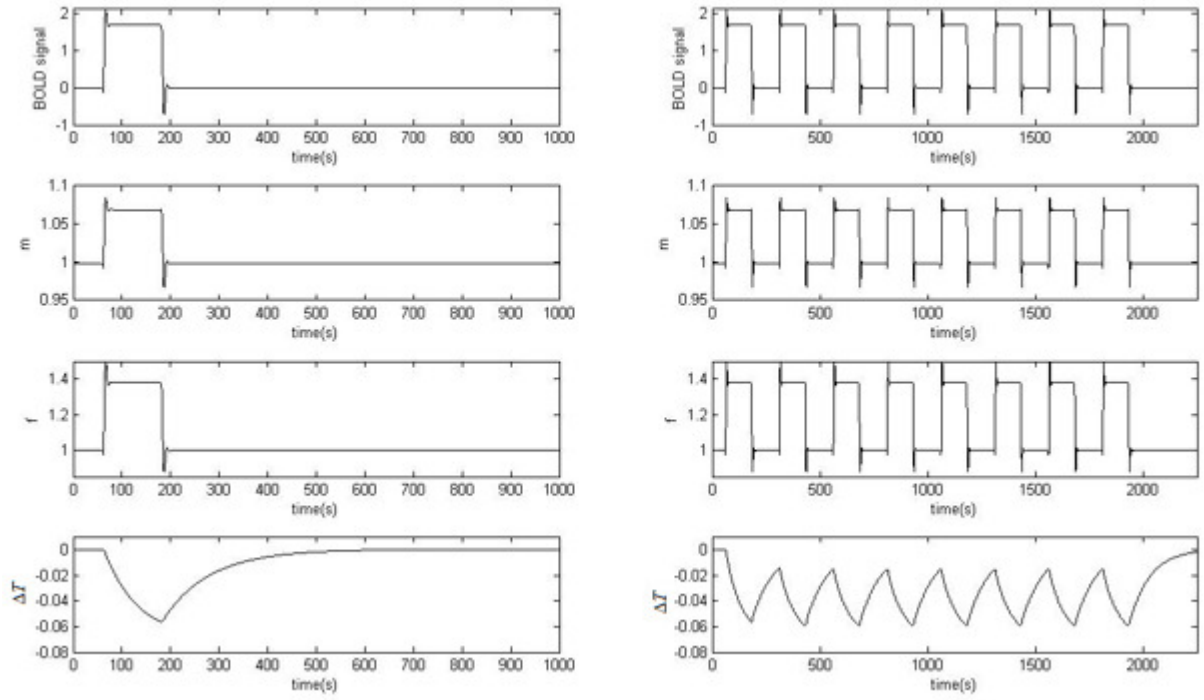

Figure 1. Temperature signals associated to positive BOLD responses. In each column from top to down: BOLD signal, $CMRO_2$ normalized to baseline (m), CBF normalized to baseline (f) and the temperature variation with respect to baseline (ΔT).

While the time characterizing BOLD changes in the brain is in the order of seconds, in the case of temperature changes is in the order of minutes (Trübel et al., 2006). This explains why while

Nature Precedings : hdl:10101/npre.2010.4772.1 : Posted 13 Aug 2010

there is no interaction between the multiples BOLD responses in Figure 1 and Figure 2, there is at the resulting temperature signals.

Finally we investigate the influence of one of the parameters, the oxygen extraction fraction at rest(E_0) on the results. Figure 3 shows ΔT for three values of E_0, finding that varying E_0 in an small range$(0.35-0.45)$ causes temperature variations one order of magnitude lower (0.002 degrees) than variations due to neuronal activity (Figures 1 and 2).

Nature Precedings : hdl:10101/npre.2010.4772.1 : Posted 13 Aug 2010

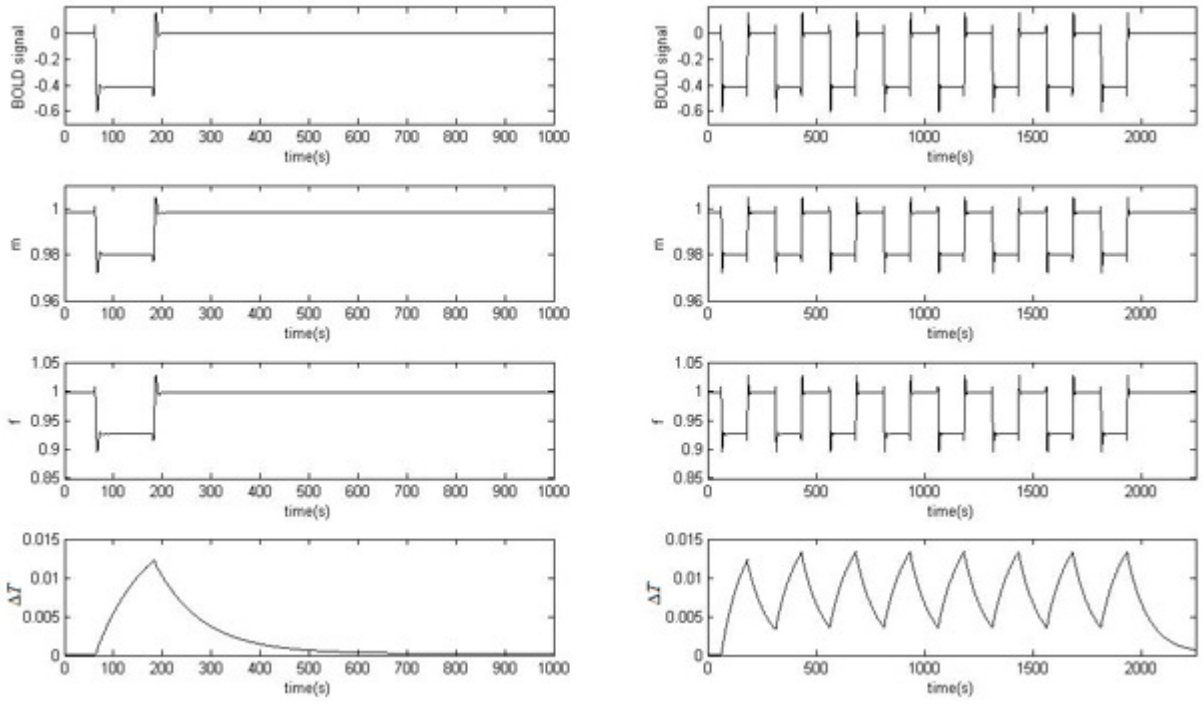

Figure 2. Temperature signal associated to negative BOLD responses. In each column from top to down: BOLD signal, $CMRO_2$ normalized to baseline (m), CBF normalized to baseline (f) and the temperature variation with respect to baseline (ΔT).

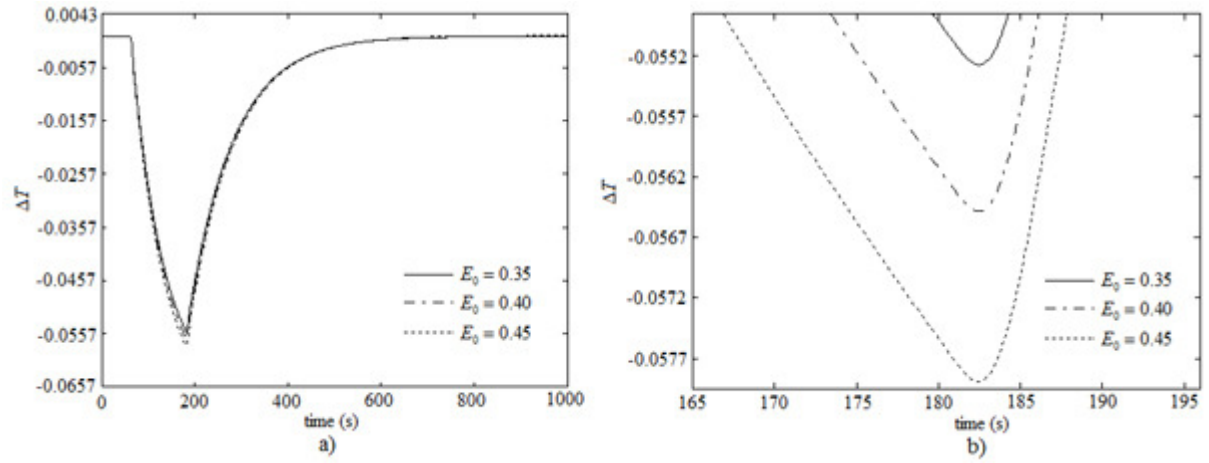

Figure 3. Influence of the oxygen extraction fraction ate rest (E_0) on the temperature. a) ΔT is plotted for three values of E_0: 0.35, 0.40 and 0.35. b) An augmented detail of b).

3.2 From real BOLD data to brain temperature maps

The real BOLD dataset was obtained from the Wellcome Department of Imaging Neuroscience, Institute of Neurology, University College London (http://www.fil.ion.ucl.ac.uk/spm/data/#epoch) and is described in Büchel and Friston (1997). The experiment was performed on a 2 Tesla Siemens VISION scanner. Contiguous multislice T2*–weighted fMRI images were obtained with a TR of 3.22 s. The original data had 32-3 mm slices covering 9.6 cm of the cortex and extending to the upper cerebellum. Subjects were scanned during four runs, each lasting 5 min 22 s. One hundred image volumes were acquired in each run. The first 10 volumes of each run were discarded to allow stabilization of the BOLD signal. Each condition lasted 10 scans or 32.2 seconds.

In this work, image processing and statistical analysis of the BOLD dataset were carried out using SPM2 (http://www.fil.ion.ucl.ac.uk/spm). A structural MRI acquired using a standard three dimensional T1 weighted sequence (1x1x3 mm^3 voxel size) was co-registered to the

Nature Precedings : hdl:10101/npre.2010.4772.1 : Posted 13 Aug 2010

T2*−weighted. All the images were spatially normalized to a standard template and the data were smoothed using a 6 mm full width at half maximum isotropic Gaussian kernel.

Using the normalized T1 image, a brain mask was created and BOLD signals for the mask points were extracted from previously T2* processed images. Then, CBF, $CMRO_2$ and Temperature signals were calculated for each voxel in the mask, using expressions (6) and (12)-(16). For each variable (CBF, $CMRO_2$ and Temperature) the calculated temporal signals were saved as a new image set.

Data activation statistical analysis on BOLD, CBF, $CMRO_2$ and Temperature image sets were performed by modeling the different conditions ('attention to motion', 'no attention to motion', 'fixation' and 'stationary') as reference waveforms in the context of the general linear model as employed by SPM2. To identify brain regions important in early visual processing, the comparison between conditions involving visual motion ('attention to motion' and 'no attention to motion') and 'fixation' was employed.

Figure 4 displays the BOLD data (first row) and the corresponding ΔT calculated with our method (second row) at four time instants: 4.83 min, 9.66 min, 14.49 min and 19.32 min. As shown in the legend, the calculated ΔT values $(-0.15:0.1)$ are within the experimentally observed range. Figure 5 shows the activated regions ($P < 0.001$, Bonferroni corrected) obtained from the statistical analysis of BOLD, f, m and ΔT data (labelled A, B, C, and D, respectively). For this dataset we obtained that f and m present similar activation patterns than the original BOLD data (i.e. activations mainly localized on visual regions V1, V2 and V5/MT). Nevertheless, we found temperature responses to be more localized than the BOLD, f and m responses (i.e. activations mainly localized on region V2).

Nature Precedings : hdl:10101/npre.2010.4772.1 : Posted 13 Aug 2010

Nature Precedings : hdl:10101/npre.2010.4772.1 : Posted 13 Aug 2010

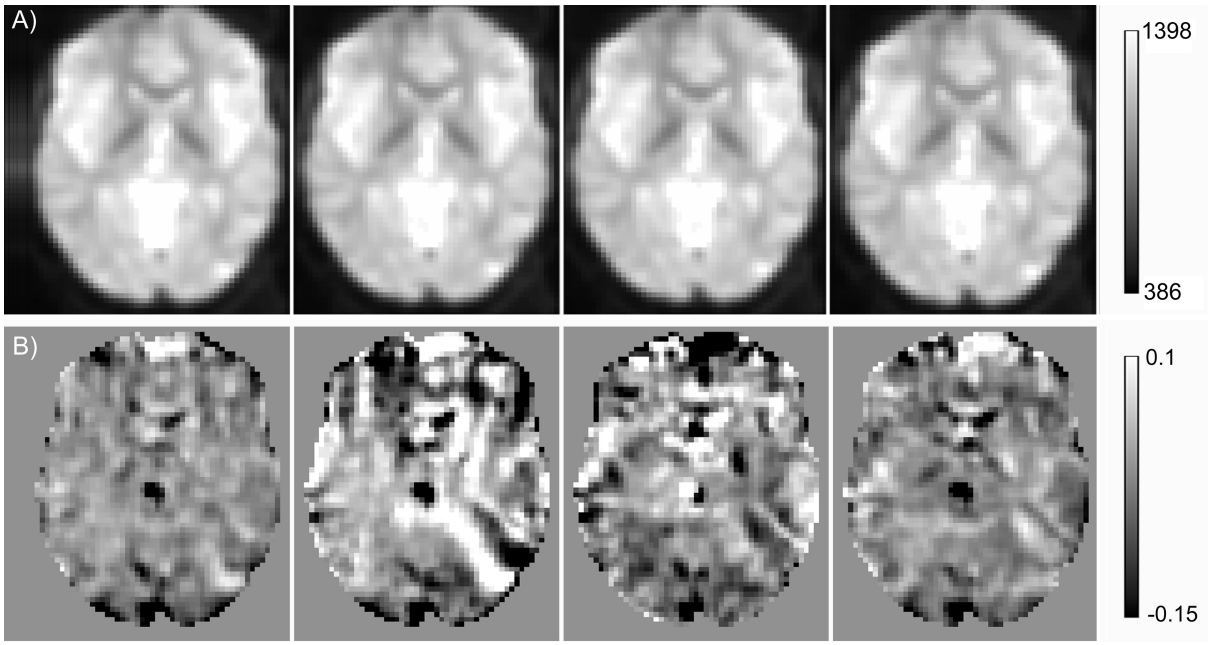

Figure 4. Temperature maps obtained from an actual BOLD dataset at four time instants: 4.83 min, 9.66 min, 14.49 min and 19.32 min. A) original BOLD dataset. B) Temperature variations.

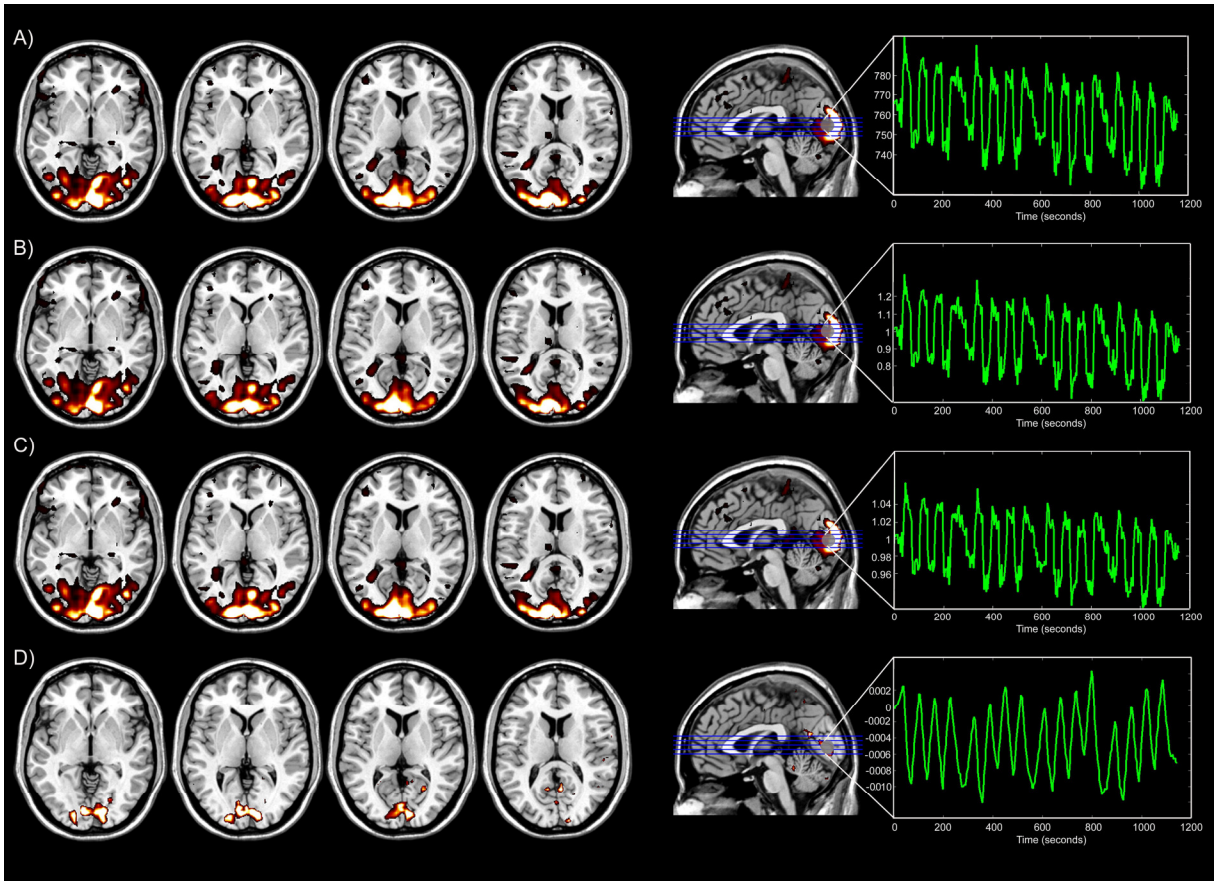

Figure 5. Activated maps obtained from the statistical analysis of the maps shown in Figure 4 ($P < 0.001$, Bonferroni corrected). A) BOLD, B) CBF normalized to baseline (f), C) $CMRO_2$ normalized to baseline (m), D) temperature variation with respect to baseline (ΔT). At the end of each row a time series extracted from the activated region is shown.

4. Discussion

In this paper we presented a theoretical framework for obtaining CBF, $CMRO_2$ and temperature responses from registered BOLD signals. This is could have potential clinical applications, as conventional methods for measuring brain temperatures require invasive probes and can monitor only one or a few locations simultaneously (Le Bihan, 1995). Using simulated BOLD data we confirmed that PBRs are linked to decreases in brain temperature, whereas NBRs are associated to temperature increases. We also demonstrated that stimulations paradigms producing multiple non-interacting BOLD responses can produce interacting temperature responses, due to the slower temporal dynamics of temperature changes. In addition, we converted real BOLD data (Büchel and Friston, 1997) into CBF, $CMRO_2$ and temperature datasets. The calculated ΔT values $(-0.15:0.1)$ are within the range experimentally observed, being smaller than the ones reported in Yablonskiy et al. (2000) and consistent with the more moderate values obtained by Gorbach et al. (2003).

Interestingly, the data analysis found that statistically significant temperature variations are more localized than BOLD activations, failing to show activations activation in brain areas where it is well known that electrical activity occurs, such as V5 bilaterally. Thus the most parsimonious interpretation of this result is that temperature data provide a less sensitive mapping of brain activity tan fMRI. This result also opens questions about the nature of the information processing

Nature Precedings : hdl:10101/npre.2010.4772.1 : Posted 13 Aug 2010

and the underlying vascular network in visual areas that give rise to the difference in temperature found here (Figures 4 and 5).

In the present paper, temperature responses were obtained by solving numerically (fourth order Runge-Kutta method) a non-autonomous differential equation that depends on the BOLD signal (see (14)-(16)). An alternative to solving this differential equation is to numerically calculate two integrals (see (17)-(18)) with a quadrature method. In the case of our simulated data, which was generated with a temporal resolution of $0.1s$, both alternatives gave the same result (not shown here). Nevertheless, actual BOLD signals have a poorer temporal resolution. For data simulated with $1-3s$ temporal resolution we found the Runge-Kutta method to have better accuracy than quadrature methods like trapeze and Simpson. Finding a more efficient numerical method is a topic for future research.

The method proposed here deals only with the temporal dynamics of the temperature. For obtaining the spatial distribution in the brain (temperature maps as shown in Figure 4) we calculate the temperature voxel by voxel. For modeling the spatial distribution of brain temperature, partial differential equations need to be employed (Collins et al., 2004; Sustanskii and Yablonskiy, 2006). The oxygen limitation model (Buxton and Frank, 1997) and the model for the BOLD signal change (Davis et al., 1998) are also temporal models. Then, the spatial correlations in CBF, $CMRO_2$ and temperature maps are forced by correlations in the BOLD signals, and not due to model design.

In the calculations presented here, we have assumed that the parameters (see Table 1) do not vary across the brain tissue. Nevertheless, it has been reported (Dunn et al., 2005) a slight spatial dependence in the power law coefficient (α) relating changes in CBF and cerebral blood volume (CBV). Additionally, the oxygen consumption at rest $\left(CMRO_2|_0\right)$ should be affected by

Nature Precedings : hdl:10101/npre.2010.4772.1 : Posted 13 Aug 2010

the inhomogeneities found in cortical tissue. That is, the motor cortex, for example, has a relatively sparse population of neurons, while sensory cortices tend to be more densely populated than the average. Furthermore, even within a given cytoarchitectonic region neuronal densities vary considerably (Abeles, 1991). $CBF\big|_0$ should also have spatial variations, as we know that vascular density is area specific (Weber et al., 2008). Nevertheless, despite these spatial variability in oxygen consumption and blood flow, there is a relatively uniformity of E_0 across the brain (Gusnard and Raichle, 2001). Using simulations we found that ΔT doesn't change appreciably in the E_0 range: $0.35:0.45$ (see Figure 3).

In this work, by using the oxygen limitation model we have assumed a tight coupling between blood flow and oxygen consumption. Thus, it is important to note that experimental evidences suggest that energy demand does not directly control *CBF* increases (Attwell and Iadecola, 2002), and in fact global changes of *CBF* independent of local energy needs have been found (Reis and Golanov, 1997). Nevertheless, changes in *CBF* do correlate with oxygen usage during functional activation (Hoge et al., 1999). Thus, the oxygen limitation model is used here only as a practical way of coupling *CBF* and oxygen consumption, without deepening in the complex nature of that link.

Finally, our model is deterministic. Nevertheless, several studies have shown the importance of the physiological noise contribution to fMRI signal fluctuations (Biswal et al., 1995; Krüger and Glover, 2001). Thus, future refinements of the present model should include physiological noise.

Nature Precedings : hdl:10101/npre.2010.4772.1 : Posted 13 Aug 2010

Acknowledgements

RCS was partially supported by the *MNI Center of Excellence in Commercialization and Research* postdoctoral fellowship.

References

Abeles, M,. 1991. Corticonics: Neural Circuits of the Cerebral Cortex, Cambridge University Press.

Attwell, D., and Iadecola, C., 2002. The neural basis of functional brain imaging signals. Trends in Neurosciences 25, 621-625.

Babajani, A., Soltanian-Zadeh, H., 2006. Integrated MEG/EEG and fMRI model based on neural masses. IEEE Trans Biomed Eng 53, 1794-1801.

Babajani, A., Soltanian-Zadeh, H., Moran, J. E., 2008. Integrated MEG/fMRI model validated using real auditory data. Brain Topogr 21, 61–74.

Bandettini, P. A., Wong, E. C., Hinks, R. S., Tikofsky, R. S., Hyde, J. S. 1992. Time course EPI of human brain function during task activation. Magn Reson Med 25, 390 –397.

Biswal, B., Yetkin, F. Z., Haughton, V. M., Hyde, J. S., 1995. Functional connectivity in the motor cortex of resting human brain using echo-planar MRI. Magnetic resonance in medicine 34, 537-541.

Blockley, N. P., Francis, S. T., Gowland, P. A., 2009. Perturbation of the BOLD response by a contrast agent and interpretation through a modified balloon model. NeuroImage 48, 84-93.

Nature Precedings : hdl:10101/npre.2010.4772.1 : Posted 13 Aug 2010

Nature Precedings : hdl:10101/npre.2010.4772.1 : Posted 13 Aug 2010

Büchel, C., and Friston, K., 1997. Modulation of Connectivity in Visual Pathways by Attention: Cortical Interactions Evaluated with Structural Equation Modelling and fMRI: Cerebral Cortex 7, 768-778.

Buxton, R. B., and Frank, L. R., 1997. A model for the coupling between cerebral blood flow and oxygen metabolism during neural stimulation. J. Cereb. Blood Flow Metab 17, 64-72.

Buxton, R. B., Wong, E. C., and Frank, L. R., 1998. Dynamics of blood flow and oxygenation changes during brain activation: The Balloon model. Magn. Reson. Med 39, 855– 864.

Buxton, R. B., Uludag, K., Dubowitz, D.J, Liu, T. T., 2004. Modeling the hemodynamic response to brain activation. NeuroImage 23, S220-S223.

Collins, C. M., Smith, M. B., Turner, R., 2004. Model of local temperature changes in brain upon functional activation. J Appl Physiol 97: 2051–2055.

Corless, R. M., Gonnet, G. H., Hare, D. E. G., Jeffrey, D. J., and Knuth, D. E., 1996. On the Lambert W function. Adv. Computational Maths 5, 329 – 359.

Davis, T., Kwong, K., Weisskoff, R., Rosen, B., 1998. Calibrated functional MRI: mapping the dynamics of oxidative metabolism. Proc. Natl. Acad. Sci. USA 95, 1834–1839.

Dunn, A. K., Devor, A., Dale, A. M., Boas, D. A., 2005. Spatial extent of oxygen metabolism and hemodynamic changes during functional activation of the rat somatosensory cortex. NeuroImage 27, 279-290.

Frahm, J., Bruhn, H., Merboldt, K. D., Hanicke, W., 1992. Dynamic MR imaging of human brain oxygenation during rest and photic stimulation. J Magn Reson Imaging 2, 501–505.

Friston K.J, Mechelli A, Turner R, Price C. J., 2000. Nonlinear responses in fMRI: The Balloon model, Volterra kernels, and other hemodynamics. NeuroImage 12, 466-477.

Nature Precedings : hdl:10101/npre.2010.4772.1 : Posted 13 Aug 2010

Friston, K. J., Harrison, L., Penny, W., 2003. Dynamic causal modeling. Neuroimage 19, 1273-1302.

Gorbach, A.M., 1993. Infrared imaging of brain function. Adv Exp Med Biol 333, 95–123.

Gorbach A. M., Heiss J., Kufta C., Sato S., Fedio P., Kammerer W. A., Solomon J., Oldfield E. H ., 2003. Intraoperative infrared functional imaging of human brain. Ann Neurol 54, 297–309.

Gusnard, D. A., and Raichle, M. E., 2001. Searching for a baseline: functional imaging and the resting human brain. Nature Review Neuroscience 2, 685-694.

Hayward, J. N., and Baker, M. A., 1968. Role of cerebral arterial blood in the regulation of brain temperature in the monkey. Am. J. Physiol. 215, 389–402.

Hindman, J. C., 1966. Proton resonance shift of water in the gas and liquid states. J. Chem. Phys. 44, 4582–4592.

Hoge, R. D., Atkinson, J., Gill, B., Crelier, G. R., Marrett, S., and Pike, G. B., 1999. Linear Coupling Between Cerebral Blood Flow and Oxygen Consumption in Activated Human Cortex. Proc. Natl. Acad. Sci. USA 96, 9403-9408.

Hyder, F., Shulman, R. G., Rothman, D. L., 1998. A model for the regulation of cerebral oxygen delivery. J Appl Physiol 85, 554–564.

Kwong, K. K., Belliveau, J. W., Chesler, D. A., Goldberg, I. E., Weisskoff, R. M., Poncelet, B. P., Kennedy, D. N., Hoppel, B. E., Cohen, M. S., Turner, R. 1992. Dynamic magnetic resonance imaging of human brain activity during primary sensory stimulation. Proc Natl Acad Sci U S A 89, 5675–5679.

Krüger, G., Glover, G. H., 2001. Physiological Noise in Oxygenation-Sensitive Magnetic Resonance Imaging. Magnetic Resonance in Medicine 46, 631–637.

Kuroda, K., Suzuki, Y., Ishihara, Y. & Okamoto, K., 1996. Temperature mapping using water proton chemical shift obtained with 3D-MRSI: Feasibility in vivo. Magn. Reson. Med 35, 20–29.

LaManna, J. C., McCracken, K. A., Patil, M., Prohaska, O. J., 1989. Stimulus-activated changes in brain tissue temperature in the anesthetized rat. Metabol Brain Dis 4, 225–237.

Le Bihan, D., 1995. Diffusion and perfusion magnetic resonance imaging, edited by D. Le Bihan. Raven Press, Ltd. New York.

McElligott, J. G., Melzack, R., 1967. Localized thermal changes evoked in the brain by visual and auditory stimulation. Exp Neurol 17, 293–312.

Melzack, R., Casey, K. L., 1967. Localized temperature changes evoked in the brain by somatic stimulation. Exp Neurol 17, 276–292.

Ogawa, S., Tank D. W., Menon, R., Ellermann, J. M., Kim, S., Merkle, H and Ugurbil, K. ,1992. Intrinsic signal changes accompanying sensory stimulation: functional brain mapping with magnetic resonance imaging. Proc. Natl. Acad. Sci. USA 89: 5951-5955.

Parker, D. L., Smith, V., Sheldon, P., Crooks, L. & Fussel, L., 1983. Temperature distribution measurements in two-dimensional NMR imaging. Med. Phys. 10**,** 321–325.

Pennes, H. H., 1948. Analysis of tissue and arterial blood temperature in the resting human forearm. J. Appl. Physiol 1, 93–122.

Reis, D. J. and Golanov, E. V., 1997. Autonomic and vasomotor regulation. Int. Rev. Neurobiol. 41, 121–149.

Riera, J., Wan, X., Jimenez, J. C., Kawashima, R., 2006. Nonlinear local electro-vascular coupling. Part I: A theoretical model. Human Brain Mapping 27, 896-914.

Nature Precedings : hdl:10101/npre.2010.4772.1 : Posted 13 Aug 2010

Riera, J., Jimenez, J. C., Wan, X., Kawashima, R., Ozaki, T., 2007. Nonlinear local electro-vascular coupling. Part II: From data to neuronal masses. Human Brain Mapping 28, 335-354.

Serota, H. M, Gerard, R. W. (1938) Localized thermal changes in the cats brain. J Neurophysiol 1, 115–24.

Shevelev, I. A., 1998. Functional imaging of the brain by infrared radiation (thermoencephaloscopy). Prog. Neurobiol. 56, 269–305.

Shevelev, I. A., Tsicalov, E. N., Gorbach, A. M., Budko, K. P., Sharaev, G. A. Thermoimaging of the brain., 1993. J Neurosci Methods 46, 49-57.

Shevelev, I. A., Tsicalov, E. N., 1997. Fast thermal waves spreading over the cerebral cortex. Neuroscience 76, 531–540.

Shmuel, A., Yacoub, E., Pfeuffer, J., Van de Moortele, P., Adriany, G., Hu, X., Ugurbil, K., 2002. Sustained negative BOLD, blood flow and oxygen consumption response and its coupling to the positive response in the human brain. Neuron 36, 1195–1210.

Sirotin, Y. B and Das, A., 2009. Anticipatory hemodynamic signals in sensory cortex not predicted by local neuronal activity. Nature 457, 475-480.

Sotero, R. C., Trujillo-Barreto, N. J., 2007. Modelling the role of excitatory and inhibitory neuronal activity in the generation of the BOLD signal. NeuroImage 35, 149-165.

Sukstanskii, A., Yablonskiy, D. A., 2006. Theoretical model of temperature regulation in the brain during changes in functional activity. PNAS 103, 12144–12149.

Takuya, H., Watabe, H., Kudomi, N., Kim, K. M., Enmi, J. I., Hayashida, K., Iida, H., 2003. A theoretical model of oxygen delivery and metabolism for physiological interpretation of quantitative cerebral blood flow and metabolic rate of oxygen. J. Cereb. Blood Flow Metab 23, 1314-1323.

Nature Precedings : hdl:10101/npre.2010.4772.1 : Posted 13 Aug 2010

Trübel, H. K. F., Sacolick, L. I., Hyder, F., 2006. Regional temperature changes in the brain during somatosensory stimulation. J Cereb Blood Flow Metab 26, 68–78.

Vafaee, M. S., Gjedde, A., 2000. Model of blood-brain transfer of oxygen explains nonlinear flow- metabolism coupling during stimulation of visual cortex. J Cereb Blood Flow Metab 20, 747–754.

Weber, B., Keller, A. L., Reichold, J., Logothetis, N., 2008. The microvascular system of the striate and extrastriate visual cortex of the macaque. Cerebral Cortex 18, 2318-2330.

Yablonskiy, D. A., Ackerman, J. J. H., Raichle, M. E.., 2000. Coupling between changes in human brain temperature and oxidative metabolism during prolonged visual stimulation. PNAS 97, 7603–7608.

Zheng, Y., Martindale, J., Johnston, D., Jones, M., Berwick, J., Mayhew, J., 2002. A model of the hemodynamic response and oxygen delivery to brain. Neuroimage 16, 617-637.

Nature Precedings : hdl:10101/npre.2010.4772.1 : Posted 13 Aug 2010